Investigation of transient chill down phenomena in tubes using liquid nitrogen

Investigation of transient chill down phenomena in tubes using liquid nitrogen

A.K. Shukla[1,2], Arunkumar Sridharan[2] and M.D. Atrey[2,†]

[1] ISRO Propulsion Complex, Mahendragiri, Tamilnadu, India 627133
[2] Indian Institute of Technology Bombay, Mumbai, Maharashtra, India 400076

[†] matrey@iitb.ac.in

Abstract: Chill down of cryogenic transfer lines is a crucial part of cryogenic propulsion as chill down ensures transfer of single phase fluid to the storage tanks of cryogenic engines. It also ensures single phase liquid flow at the start of the engine. Chill down time depends on several parameters such as length of the pipe, pipe diameter, orientation, mass flux etc. To understand the effect of these parameters, experiments are carried out in a set up designed and fabricated at Indian Institute of Technology Bombay using tubes of two different diameters. Experiments are conducted at different inlet pressures and mass flow rate values to understand their effect. Two different pipe sizes are taken to study the effect of variation in diameter on chill down time and quantity of cryogen required. Different orientations are taken to understand their effect on the chill down time, heat transfer coefficient and critical heat flux for the same inlet pressure and mass flux. Pipe inner wall temperature, heat transfer coefficient for different boiling regimes and critical heat flux are calculated based on measured outer surface temperature history for each case.
A one dimensional energy conservation equation is solved for transient chill down process considering constant mass flux and inlet pressure to predict the chill down time. Temperature variation during chill down obtained from the numerical simulations are compared with the measured temperature history.

Keywords: Chill down, Liquid Nitrogen, Boiling curve, heat flux, Film boiling

1. Introduction

Cryogenic fluids are widely used in various industries including space industry. Different cryogenic fluids find their applications in cryosurgery, preservation of tissues and blood, fuel cells, medical industry, health supporting systems etc. Along with this, cryogenic propulsion is a very prominent area of application of cryogenic fluids. Chill down of cryogenic storage tanks, cryogenic transfer lines, cryogenic engine and its piping form techniques essential in the area of cryogenic propulsion [1].

Chill down can be referred to as first stage of cryogenic fluid transfer. For any cryogenic application, the first objective is to transfer cryogenic fluid with minimum consumption and losses. In order to minimize the losses and consumption, the process needs to be optimized. An efficient chill down ensures transfer of single phase fluid from one component to another component in a system. Knowledge of chill down gives an advantage to the designer for sizing the piping system and associated circuits for low temperature applications. When cryogenic fluid enters a tube or pipeline, which is in thermal equilibrium with the ambient, vigorous boiling of the fluid results. As specific volume ratio for gas to liquid is very high for cryogenic fluids, boiling results in a rapid increase in the volume of the fluid which the pipe may not be able to vent out instantaneously. This increase in volume results in high pressure surges, back flow and high thermal gradients inside the pipeline. As

the pressure in the pipeline increases, it pushes the fluid back to the vessel and there is no flow of fluid from the vessel to the pipeline until pressure in the pipeline reduces to a value less than the pressure in the vessel. This process of boiling and phase change continues until the pipe comes in thermal equilibrium with the fluid. This phenomenon is referred as line "chill down" or line cool down [2]. The phenomenon of chill down is characterized by large temperature differences, rapid transients and pressure fluctuations.

Chill down studies started in the late 1960's and one of the initial studies was carried out by Burke et. al. [3] in which, different parameters such as driving pressure at the line, line heat in leak, line thermal mass, effect of concentrated mass etc. were studied. A model was also proposed to estimate the chill down time of pipe line. Fourier series was used to study the chill down of concentrated mass considering it to be a semi-infinite slab. In a series of latest papers by Darr et. al. [1, 4] effect of different parameters such as mass flux, equilibrium quality, inlet subcooling, flow direction etc. was studied for horizontal, vertical and inclined orientations on a stainless steel 304 grade tube. A set of correlations were proposed for different boiling regimes such as film boiling, transition boiling and nucleate boiling based on experimental data for different orientations.

Jackson et. al. [5] calculated heat transfer coefficient at top and bottom of a pipe line using inverse heat transfer technique. Liao et. al. [6] considered a pseudo-steady model and developed a correlation for film boiling for a horizontal tube. He considered liquid wave front speed as constant and remained same as that of bulk liquid speed. Johnson et. al. [7] discussed the chill down of a horizontal and inclined orientation and reported that at an optimum angle, chill down time is minimum and effect of inclination is more dominant on small mass flow rates. Hu et. al. [8] discussed the effect of flow direction on chill down in case of a vertical pipe and studied the variation of heat transfer coefficient, chill down etc. with flow direction. Hartwig et. al. [9] discussed the effect of Reynolds number and thermophysical properties on chill down and reported that at high Reynolds number, Leidenfrost temperature is high. They also concluded that hydrogen instantly by passes the film boiling regime thus reducing the chill down time drastically. Majumdar et. al. [10] showed the effect of subcooled and saturated liquid on chill down for liquid nitrogen and liquid hydrogen. They inferred that chill down time was less for liquid hydrogen than for liquid nitrogen. They further observed that chill down time will be less for a subcooled liquid as compared with the saturated liquid.

In the present study, a one dimensional (1-D) transient model is solved to predict the temperature variation with respect to time at a given location. In addition, experiments are conducted for a wide range of mass flow rates to see the effect of mass flux on the chill down. Upward flow experiments are also carried out on two different line sizes at several different orientations.

2. One dimensional numerical model

A one dimensional numerical model is developed similar to that given by Darr et. al. [11]. In this model, conduction equation is solved to predict the temperature profile at a given location. Control volume for this is shown in figure 1

$$\rho_s c_{p,s} \frac{\partial T_w}{\partial t} = \frac{\partial}{\partial z}\left(k_s \frac{\partial T_w}{\partial z}\right) + \frac{1}{r}\frac{\partial}{\partial r}\left(r k_s \frac{\partial T_w}{\partial r}\right) + \frac{1}{r}\frac{\partial}{\partial \Phi}\left(\frac{k_s}{r}\frac{\partial T_w}{\partial \Phi}\right) + \dot{q}_{conv}(z) + \dot{q}_{parasitic}(z) \qquad (1)$$

Here 's' and 'w' represents properties of solid material and the wall. ρ is density, c_p is the specific heat at constant pressure, k is the thermal conductivity and T is temperature. r, z and ϕ are symbols for a cylindrical coordinate system. Here $\dot{q}_{conv}(z)$ represents the heat removed from the wall by the fluid and $\dot{q}_{para}(z)$ represents the heat in leak coming to the test section from the surrounding and consist of radiation heat flux and convective heat flux at the outer surface. Radiation heat flux is calculated using Stefan Boltzmann law [12] and heat flux at the outer surface is calculated using Churchill and Chu correlation [12] for natural convection over a horizontal cylinder. Subscript 'amb' is used for ambient and 'sur' is used for surface of the insulation. D_o is the outer diameter of the insulation and h_{out} is the heat transfer coefficient at the outer surface and h_{conv} is the heat transfer coefficient for inner surface.

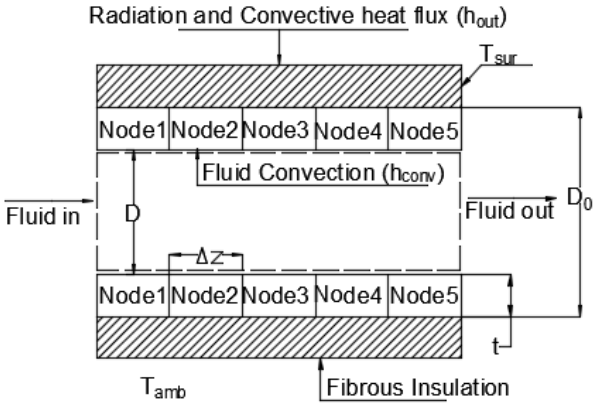

Figure 1. Control volume for numerical simulation.

It is assumed that for small line sizes, temperature gradients in radial and azimuthal directions are small compared with the temperature gradient in the axial direction and hence neglected. With these assumptions, equation (1) is reduced to the form given in equation (2).

$$\rho_{sC_{p,s}} \frac{\partial T_w}{\partial t} = \frac{\partial}{\partial z}\left(k_s(T)\frac{\partial T_w}{\partial z}\right) + \dot{q}_{conv}(z) + \dot{q}_{parasitic}(z) \tag{2}$$

It is also assumed that the mass flow rate is constant and pressure distribution during chill down is independent of time. In case of horizontal lines, fluctuations in mass flow rate and pressure are very small and can be neglected. This equation is discretized using second order central difference scheme for axial term and first order implicit formulation for temporal term.

Tri-diagonal matrix obtained from discretized form of equation (2) at every node is solved using Thomas algorithm. Boundary conditions to solve the equation are, (i) at inlet first node temperature is equal to the saturation temperature of the fluid during the trial and (ii)at exit heat flux at the last node is same as that of node prior to it. In order to calculate the equilibrium quality 'xe' and enthalpy 'h' at a node equation (3) and (4) are used.

$$h_i^j = h_{i-1}^j + q_{conv,i}^{j-1}/G \tag{3}$$

$$x_{e_i}^{\ j} = \left(h_i^j - h_l\right)/h_{lv} \tag{4}$$

$T_{Leidenfrost}, T_{ONB}, q_{NB}\ and\ q_{CHF}$ are calculated for the given mass flow rate and pressure. The values of wall temperature and heat flux are compared against the respective values to distinguish among different boiling regimes. Thus the appropriate correlation equation (5) to (8) can be employed.

For film boiling, the modified Bromley correlation as given by equation (5) is used. For nucleate boiling and transition boiling correlation given by Darr et. al.[4] given in equation (6) and (7) are used. For single phase convection Dittus Boelter correlation as given by equation (8) is used. As most of the chill down occurs in film boiling, match of temperature profile obtained by numerical prediction depends on the accuracy of film boiling correlation for this case. Various correlations are as given :

$$h_{FB} = 0.62\left[k_v^3 \frac{\rho_v g(\rho_l-\rho_v)(h_{lv}+0.4C_{p,v}\Delta T)}{L_h \mu_v \Delta T}\right]^{0.25} \tag{5}$$

Here $L_h = \text{minimum}\,(L_{h1}, L_{h2})$, $L_{h1} = \frac{d_i}{2}$, $L_{h2} = 2\pi\left[\frac{\gamma_{lv}}{g(\rho_l-\rho_v)}\right]$ $and\ \Delta T = T_{wall} - T_{sat}$

$$h_{NB} = 22.8\, Re_l^{-0.332} Ja_l^{-0.254} h_{DB} \tag{6}$$

$$h_{TB} = 0.41\left(\frac{T_i - T_{l,sat}}{T_{wet} - T_{l,sat}}\right)^{0.0038} h_{NB} \quad (7)$$

$$h_{DB} = 0.023 Re_l^{0.8} Pr_l^{0.4} \left(\frac{k_l}{d}\right) \quad (8)$$

Here γ represents surface tension, 'l' and 'v' are for liquid and vapour phase respectively.

The solution is checked for convergence and grid independence. Pressure drop along the length of test section is calculated using homogenous flow model. As the change in quality is little along the length of the test section, pressure drop calculated from the homogenous flow model gives a close match with experimental values. Based on this pressure drop, pressure at each node is calculated and gets revised at every time step based on equilibrium quality of previous time step.

3. Experimental setup and instrumentation

A schematic of the test set up is shown in figure 2. The experimental test set up consists of a liquid nitrogen Dewar. High pressure gaseous nitrogen (GN_2) cylinder is used to pressurize the LN_2 Dewar. Two test sections are made of seamless stainless steel 304 tube, one of 13.5 mm inside diameter and 1.2 mm wall thickness (size S1) and other of 21 mm inside diameter and 2 mm wall thickness (size S2). Polyurethane foam sheet is used for insulation and two layers of this sheet is wrapped around the test section. Experiments are conducted for different mass flow rates and inlet pressure values using liquid nitrogen.

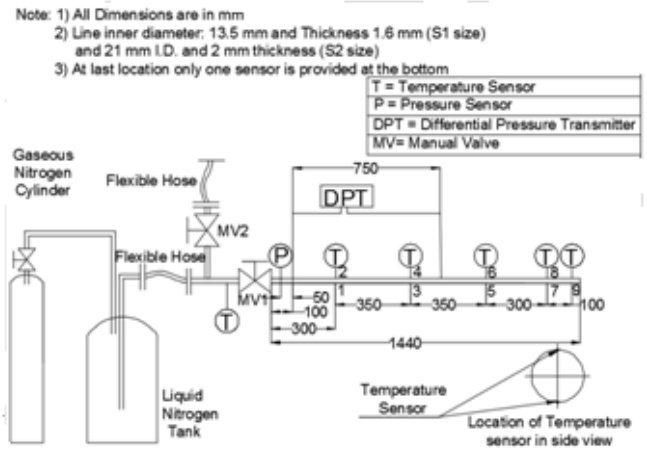

Figure 2. Schematic of the test setup with instrumentation details of the test section.

Surface temperature sensors (Pt 100) are provided at 5 locations along the length of the test section to measure outer surface temperature. At one axial location, two surface temperature sensors are provided, one at the bottom and other at the top of the cross section. It is ensured that the response time for all the sensors are the same. Inlet pressure and differential pressure are measured during the trials using a piezoelectric pressure transducer and differential pressure transmitter respectively. For doing vertical trials, test section is mounted above the manual valve MV2. Flow rate is measured using digital weighing machine

4. Results and discussion

Experimental results and comparison with numerical results are presented in this section.

4.1 Variation of temperature with time

Temperature profile at three different axial location of test sections i.e. 300 mm, 650 mm and 1300 mm from inlet for both the line sizes S1 and S2 are given in figure 3 and 4 respectively at two different mass flow rates.

It may be observed that for small line size (S1) at flow rate of 10 g/s, the sensor near to the inlet of test section reaches steady state first and thereafter sensor located near the exit, whereas at high flow

rate of 66 g/s, sensor located near the exit reaches steady state prior to the sensor located near the inlet. For large line size, this kind of behavior is not observed, as for both the flow rates, mass flux (28.87 and 190.55 kg/m^{2}s for m =10 g/s and 66 g/s respectively) is relatively lower for S2.

In chill down application, when cryogen enters the pipe line, initial heat transfer takes place through film boiling and when the temperature of the wall reaches rewetting temperature [13], liquid comes into contact with the wall. Then the liquid front starts moving from the inlet along the pipe inner wall. Due to the movement of the liquid front, film boiling shifts to transition and then to nucleate boiling and finally steady state is achieved. This phenomenon happens in most of the chill down applications and the same is clear from the low flow rate temperature profile for S1 as shown in figure 3 and from the temperature profiles for both the flow rates for S2 as shown in figure 4. In case of low flow rates, most of the liquid in the test section gets converted into vapour and very small amount of liquid in the form of droplets remains in the stream. Due to this when the film breaks, liquid droplets available in the core alone come in the contact with the wall and evaporates to form the film. No major reduction in wall temperature is noticed as energy removed due to wall and liquid droplet contact is very little.

In case of high mass flow rate, only small fraction of liquid evaporates and liquid vapour mixture which is moving downstream consist of major amount of liquid in the core of the pipe and flow pattern is nearly annular. In this case, when vapour film breaks, liquid comes into contact with the wall rather than liquid droplets and high amount of energy is removed from the wall. By this time the vapour layer separates the fluid and the wall. The temperature of the wall reduces drastically as compared to any other location of the test section. In experimental trials, which are carried out at high flow rates, phenomena similar to this occur. Along with this at high flow rates, film thickness reduces towards the downstream and causes an increased rate of heat transfer at downstream location as compared with the upstream location. As a result, downstream section temperature reduces faster than that of the upstream section for high flow rate and the same is visible from the high flow rate temperature profile for S1 as shown in the figure 3.

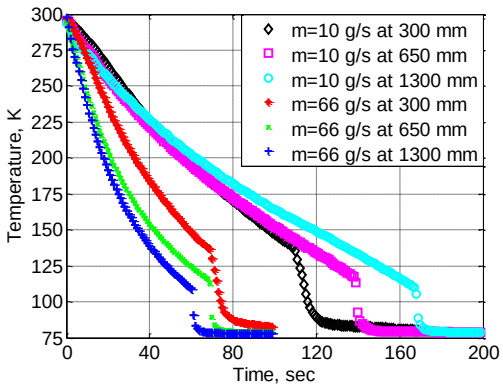

Figure 3. Variation of temperature with time for S1.

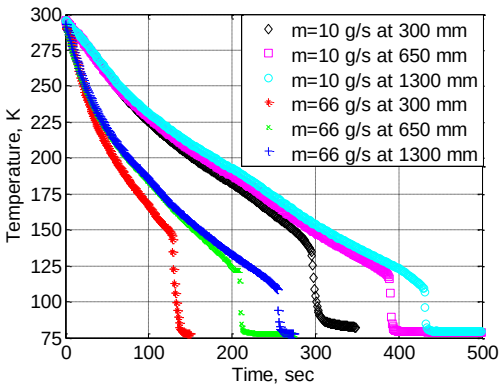

Figure 4. Variation of temperature with time for S2.

4.2 Instability at liquid vapour interface due to phase velocity

To understand the effect of the phase velocity, temperature variation for S2 is shown in figure 5. In this figure, temperature profile of the bottom temperature sensors for all the five locations is given. In this case, when liquid boils and phase change occurs, velocity of vapour increases as mixture of liquid and vapour moves downstream. At very low flow rate, near the exit of the test section, difference between liquid and vapour phase velocities is quite high and gives rise to unstable liquid vapour interface. It causes a premature rewetting which can clearly be seen from the temperature profile of the last sensor. This is also the reason for the increased rewetting temperature of the fourth sensor. As far as small line size is concerned, this phenomena is not observed as the relative difference between the phase velocities is not significant to make the interface unstable. This instability disappears with increase in flow rate and is not observed for a mass flow rate of 66 g/s.

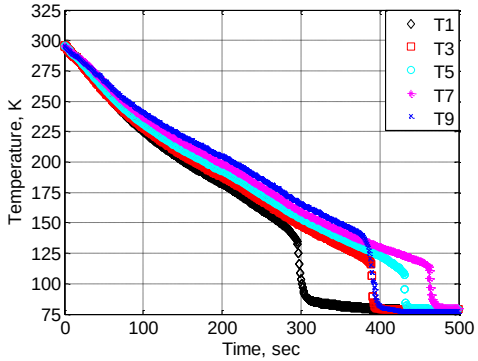

Figure 5. Variation of temperature with time at ṁ= 10 g/s for S2.

4.3 Effect of pipe orientation

To show the effect of the pipe orientation on the chill down for different line sizes, plot of temperature measured by the sensor T_9 located near exit is shown. This sensor location is selected as the effect of inclination is more pronounced at downstream locations. For S1 size, plot at orientations of 0°, 5°, 10° and 20° is given in figure 6, whereas for S2, plot at orientations of 0°, 5°, 10°, 20° and 30° is shown in figure 7. It is clear from the figure 6 that for S1 chill down time reduces with increase in orientation and reaches its minimum between orientation of 10° and 20° and thereafter chill down time starts to increase again. For line size S2, chill down time reduces with increase in orientation up to 30° and minimum chill down will occur at an orientation beyond 30°. This indicates that optimum orientation for a line size where minimum chill down time occurs is a function of line size also.

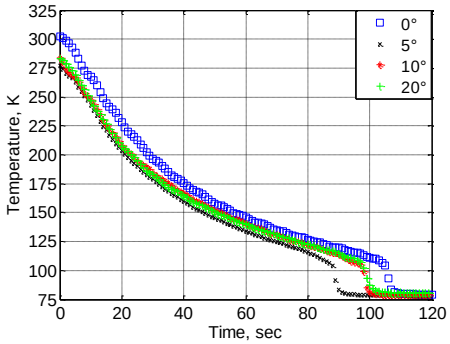

Figure 6. Variation in chill down time with orientation at $\dot{m}$ = 32 g/s for S1.

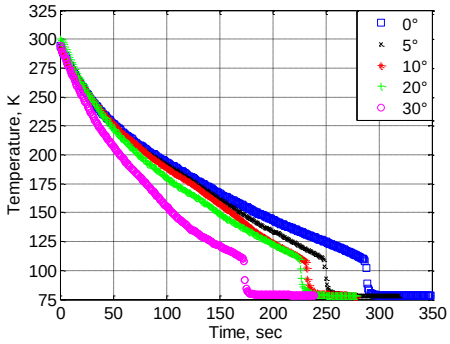

Figure 7. Variation in chill down time with orientation at $\dot{m}$ = 46 g/s for S2.

4.4 Variation of heat flux

With increase in mass flow rate, chill down time reduces. This reduction in chill down time occurs due to increase in heat transfer coefficient. Variation of heat flux for two mass flow rates of 10 g/s and 66 g/s for S1 and S2 at upstream (i.e. 300 mm from inlet) and downstream location (i.e. 1300 mm from inlet) is shown in figure 8 and 9, respectively. Heat flux is calculated using the measured surface temperature history. To calculate transient conduction heat flux and inner wall temperature, equations (9) and (10) [14] are used respectively. Total heat flux is obtained using energy balance as given by equation (11). Variation of heat flux shows that, at upstream location heat flux is more for S2 as compared with the S1. However, at downstream location, heat flux at $\dot{m} = 66\ g/s$ for S1 is of the same order as of S2.

$$T_i = T_o + \left[\frac{{r_0}^2}{4\alpha}\left\{\left(\frac{r_i}{r_o}\right)^2 - 1 - 2\,ln\left(\frac{r_i}{r_o}\right)\right\}\right]\frac{dT_0}{dt} + \left\{\frac{1}{64\alpha^2}({r_i}^4 - 5{r_o}^4) - \frac{r_o^2 r_i^2}{8\alpha^2}ln\left(\frac{r_i}{r_o}\right) - \frac{r_o^4}{16\alpha^2}ln\left(\frac{r_i}{r_o}\right) + \frac{r_o^2 r_i^2}{16\alpha^2}\right\}\frac{d^2T_o}{dt^2} \quad (9)$$

$$q_t = \rho c_p \left(\frac{r_i^2 - r_o^2}{2r_i}\right)\frac{dT_o}{dt} + \frac{(\rho c_p)^2}{k}\left\{\frac{r_i^3}{16} - \frac{r_o^4}{16r_i} - \frac{r_o^2 r_i}{4} ln\left(\frac{r_i}{r_o}\right)\right\}\frac{d^2T_o}{dt^2} + \frac{(\rho c)^3}{k^3}\left\{\frac{r_i^5}{384} - \frac{3r_o^4 r_i}{128} + \frac{3r_o^2 r_i^3}{128} - \frac{r_o^6}{384r_i} - \frac{r_o^2 r_i^3}{32} ln\left(\frac{r_i}{r_o}\right) - \frac{r_o^4 r_i}{32} ln\left(\frac{r_i}{r_o}\right)\right\}\frac{d^3T_o}{dt^3} \quad (10)$$

$$q_{conv,i} = q_{trans,i} + \left(\frac{r_o}{r_i}\right) \times (q_{conv} + q_{rad}) \quad (11)$$

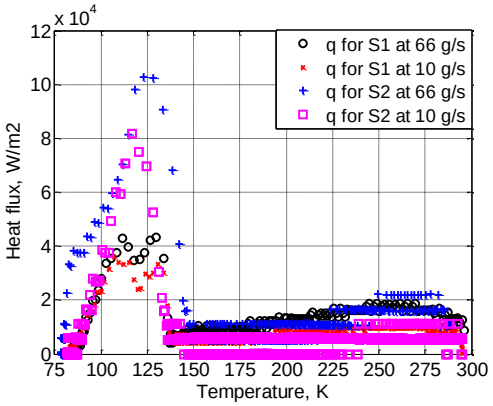

Figure 8. Variation of heat flux at upstream.

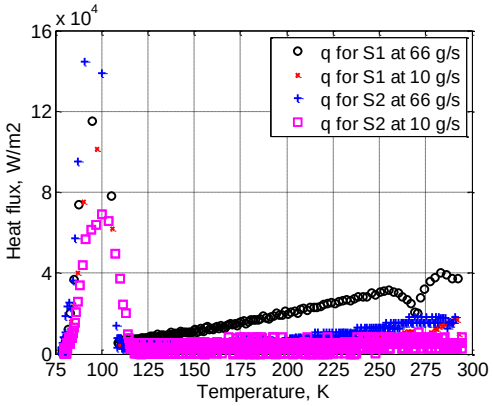

Figure 9. Variation of heat flux at upstream.

4.5 Comparison of experimental and numerical results

As described in section 3, temperature profiles for both the line sizes are compared with experiemntal results at $\dot{m}$ = 10 g/s and 66 g/s and are given in figure 10 and 11. Numerical results obtained for S1 shows a good match for low flow rate of 10 g/s whereas, for high flow rate of 66 g/s, numerical results overpredict the temperature. This could be because modified Bromley correlation is devloped for some selected fluids like absolute ethyl alcohol, benzene, carbon tetrachloride and n-hexane. As far as fluid velocities are concerned, liquid velocity at the inlet is 0.58 m/s and 0.086 m/s for high and low flow rates respectively and is within the range given in the modified Bromley correlation. Despite these limitations, numerical results and experimental results show good match for a mass flow rate of 10 g/s. The difference in temperature is visible only after rewetting point. Numerical simulation under predcited the rewetting temperature in this case whereas, for high flow rate, value of rewetting temperature obtained from numerical code is larger than the experimental value. Under prediction and over prediction of rewetting temperature is due to the local effects which occur during the experimental trials. For higher size, the prediction in the film boiling regime do not show good match with the experimental result. One more drawback of Modified Bromley correlation is that prediction of temperature in film boiling regime for both the flow rates are almost same.

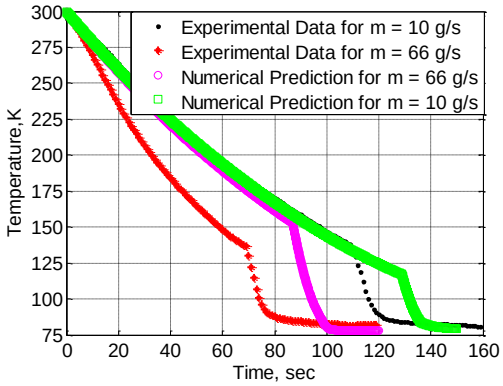

Figure 10. Experiment and numerical results for S1.

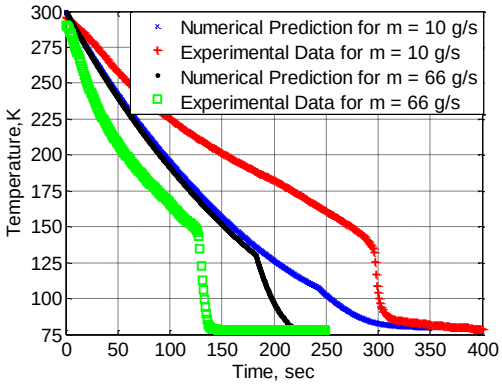

Figure 11. Experiment and numerical results for S2.

5. Summary

Results obtained from the experimental trials indicate that at very high mass flow rate, mechanism of chill down is not dominated by the movement of liquid front. The fluid velocity plays a major role and premature rewetting can occur at high flow rates. At very low flow rates near the exit, large difference in liquid and vapour phase velocity causes instability of liquid and vapour interface which also results in premature rewetting. Minimum chill down time changes with the orientation and also depends on the line size and flow rate. For very high mass flow rate, the amount of heat removed increases towards the downstream location due to increase in fluid velocity.

Comparison of experimental and numerical results shows that temperature profile obtained in the film boiling regime using modified Bromley correlation is not close to the experimental values.

References

[1] Darr S.R., Hu H., Glikin N.G., Hartwig J.W., Majumdar A.K., Leclair A.C. and Chung J.N. 2016 An experimental study on terrestrial cryogenic transfer line chilldown I. Effect of mass flux, equilibrium quality, and inlet subcooling *International Journal of Heat and Mass Transfer,* **Vol. 103**, 1225–42.

[2] Hartwig J., Hu H., Styborski J. and Chung J.N. 2015 Comparison of cryogenic flow boiling in liquid nitrogen and liquid hydrogen chill down experiments *International Journal of Heat and Mass Transfer- **88** ,* 662–73

[3] Burke J.C., Byrnes W.R., Post A.H. and Ruccia F.E. 1960 Pressurized cooldown of cryogenic transfer lines *Advances in Cryogenic Engineering* **Volume 4** 378–94.

[4] Darr S. R., Hu H., Glikin N.G., Hartwig J.W., Majumdar A.K., Leclair A.C. and Chung J.N. 2016 An experimental study on terrestrial cryogenic transfer line chilldown II. Effect of flow direction with respect to gravity and new correlation set *International Journal of Heat and Mass Transfer* **Vol. 103** 1243–60.

[5] Jackson J., Liao J., Klausner J.F. and Mei R. 2005 Transient heat transfer during cryogenic chill down *ASME Summer Heat Transfer Conference, Proceedings of HT 2005, July 17-22*

[6] Liao J., Yuan K., Mei R., Klausner J. F. and Chung J. 2015 Cryogenic chilldown model for stratified flow inside a pipe *ASME Summer H. T. Conference, Proceedings of HT 2005, July 17-22*

[7] Johnson J. and Shine S.R. 2015 Transient cryogenic chill down process in horizontal and inclined pipes *Cryogenics* **Vol. 71** 7–17.

[8] Hu H., Chung J.N. and Amber S.H. 2012 An experimental study on flow patterns and heat transfer characteristics during cryogenic chill down in a vertical pipe *Cryogenics* **Vol. 52** 268–77

[9] Hartwig J., Hu H., Styborski J. and Chung J.N. 2015 Comparison of cryogenic flow boiling in liquid nitrogen and liquid hydrogen chill down experiments *International Journal of Heat and Mass Transfer* **Vol.88** 662–73

[10] Majumdar A and Ravindran S.S. 2011 Numerical prediction of conjugate heat transfer in fluid network *Journal of Propulsion & Power* **Vol. 27**

[11] Darr S., Hu H., Hartwig J. and Majumdar A. 2015 Numerical simulation of the liquid nitrogen chill down of a vertical tube *American institute of Aeronautics and Astronautics*

[12] Cengel Y.A. and Ghajar A.J. 2015 Heat & Mass Transfer Fifth edition *McGraw Hill Education*

[13] Filipovic J., Incropera F.P. and Viskanta R. 1995 Rewetting temperature and velocity in a quenching experiment *Heat Transfer Laboratory, Purdue University*

[14] Burggraf R. 1964 An exact solution of inverse problem in heat condition theory and application *Journal of Heat Transfer*-**86** 373–82.